Journal of Scientific Research and Reports

Volume 30, Issue 10, Page 465-481, 2024; Article no.JSRR.124326
ISSN: 2320-0227

Geochemical Evaluation of the Silurian, Devonian, and Carboniferous Source Rocks at the Erawin Field, Murzuq Basin, SW Libya

Alsharef A. Albaghday [a], S. Aboglila [a*], Moustafa A. Abdullah [b], Alsedik M. A. Abousif [b], E. Farifr [c] and Mohamed H. Targhi [d]

[a] Libyan Academy, Libya.
[b] Sebha University, Libya.
[c] Azzytuna University, Libya.
[d] Mellitah Oil and Gas Company, Libya.

Authors' contributions

This work was carried out in collaboration among all authors. All authors read and approved the final manuscript.

Article Information

DOI: https://doi.org/10.9734/jsrr/2024/v30i102474

Open Peer Review History:
This journal follows the Advanced Open Peer Review policy. Identity of the Reviewers, Editor(s) and additional Reviewers, peer review comments, different versions of the manuscript, comments of the editors, etc are available here: https://www.sdiarticle5.com/review-history/124326

Original Research Article

Received: 27/07/2024
Accepted: 29/09/2024
Published: 04/10/2024

ABSTRACT

Eighty-five rock samples corresponding to the Palaeozoic formations were taken from two wells in the NC 200 Block of the Murzuq Basin. The study aimed to find out geochemical characteristics of Silurian Bir Tlacsin/Tanezzuft Formations, the Devonian Awaynat Wanin/BDS II Formations, and

**Corresponding author: E-mail: salem.aboglila@gmail.com;*

Cite as: *Albaghday, Alsharef A., S. Aboglila, Moustafa A. Abdullah, Alsedik M. A. Abousif, E. Farifr, and Mohamed H. Targhi. 2024. "Geochemical Evaluation of the Silurian, Devonian, and Carboniferous Source Rocks at the Erawin Field, Murzuq Basin, SW Libya". Journal of Scientific Research and Reports 30 (10):465-81. https://doi.org/10.9734/jsrr/2024/v30i102474.*

the Carboniferous Marar/Lower Marar Formations. Rock-Eval analysis, Total organic carbon (TOC) parameters and specific Gas Chromatography-Mass Spectrometry (GC-MS) biomarkers were applied to determine the potential hydrocarbon generation. Per se, Rocks are good sources and hold fair content of organic matter, crossing in the range of good accumulation, in which the very good source rocks have an organic carbon richness (TOC) reached of 3.7 wt%. The studied rocks are ranged from immature to late mature organic matter (OM) with total organic carbon richness (TOC) range between 0.4 – 3.7 wt%. Rock-Eval parameters S_1, S_2, S_3, Tmax, S_2/S_3, OI, PI and HI of the source rock samples have values ranged from 0.02 – 0.3, 0.22 – 6, 0.36 – 4, 423 – 443, 24= 350, 0 – 0.27 and 42 – 384 respectively. The range of hydrogen index (HI) related to oxygen index (OI) displays that all kerogen types from Type II to Type III are exist and increase with depth. The Tmax parameter is wide-ranging among studied formations, indicating different levels of organic matter maturity, from immature oil window and to late mature for the Devonian-Carboniferous and Silurian source rocks, associated with more depth. Molecular composition analysis of *n*-alkanes and other biomarkers supported the findings of Rock-Eval pyrolysis data, revealing varied hydrocarbon signatures across the formations. The Carbon isotope analysis ($\delta^{13}C$) suggested multiple sources contributing to the generated oil, including Type I to Type III kerogens.

Keywords: Murzuq basin; source rocks; potential silurian; devonian; carboniferous source rocks.

1. INTRODUCTION

The Murzuq Basin is an intracratonic basin situated on the North African Platform. It is one of several endorheic intracratonic basins of the North African platform and spans over 350,000 km^2 [1]. The current borders of the Murzuq Basin were mainly defined by erosion resulting from polyphase tectonic uplifts, with the flanks including the Tassili Plateau (Tihemboka High) to the west, the Tibesti High to the east, and the Gargaf Arch to the north (Fig. 1). All these uplifts were formed by numerous tectonic movements, ranging from the mid-Paleozoic through the Tertiary. According to Davidson et al. (2000), the Murzuq Basin is best described as an erosional remnant of a much larger Palaeozoic and Mesozoic sedimentary basin, which originally extended over much of North Africa. The Murzuq Basin is filled with a substantial sediment column ranging from the Cambrian to Quaternary in age. The sedimentary rocks in the middle part of the basin have a thickness exceeding 4000 m and consist mainly of Palaeozoic and Mesozoic sandstones and shales. The oldest Paleozoic sediments are visible on the external margins of the basin, while Mesozoic sediments form an escarpment in the middle part of the basin. Cenozoic sediments comprise over 100 m thick, mainly Paleocene marine limestone, dolomite, and marl, limited to the northern and northeastern margins of the Murzuq Basin.

The oil and gas exploration in the Murzuq basin began in the mid-1980s. compared to the extensive history of exploration of other basins in Libya, this period marked a lack of focus on the Murzuq Basin [2]. Several oil fields, such as El Sharara, Elephant, and later Erawin oilfield, have been classified as mature since the 1990s. Erawin, an onshore oil field in the southwestern part of the Murzuq Basin, was announced as an important oil discovery in late 2022 to early 2023. Known as NC 200 block, this field is operated by Zallaf Libya Oil and Gas Exploration Company in partnership with the Libyan National Oil Corporation. The NC 200 is produced from the Palaeozoic Mamuniyat formation.

1.1 Basin Infill History

Several significant tectonic phases mark the structural history of the Palaeozoic. The first of these phases is associated with the Pan-African orogeny occurring between 900–600 Ma. This movement resulted from collisions involving the West African Craton, the East Saharan Craton, and various island arcs [3-8]. The acoustic basement consists of Precambrian granitic rocks and metasediments of Mourizide Formation. Cambrian fluvial quartzites of the Hasawnah Formation unconformably overlie it. Similar facies characterize the overlying Lower Ordovician Achabiyat Formation. At the same the conformable Middle Ordovician Hawaz Formation (a reservoir target) is composed of sandy, transgressive-regressive marine sequences with significant bioturbation as shown in Fig. 2. The Middle Ordovician has been deeply incised by erosion, intense lowstand, and a late Ashgillian (Hirnantian-glacial) unconformity associated with the maximum advance of the Gondwana ice cap [9-12]. The Upper Ordovician

(Ashgillian), Melaz Shuqran, and Mamuniyat formations infill the incised valleys and rest unconformably on the Hawaz Formation (Fig. 2). The Melaz Shuqran Formation is characterized by diamictite and slumped delta front shales but is only locally present. It is overlain or overstepped by an incised cycle of coarsening up marine and fluvial-deltaic sediments in the Mamuniyat Formation (primary reservoir objective). The Ordovician section is truncated at the Taconian unconformity, which displays paleo-relief under a transgressive sequence comprising the Lower Silurian Tanezzuft Formation shales. These sediments deposited in restricted open marine conditions present organic-rich shale levels at the base, termed “hot shales,” that constituting the main source rock for the area [12,13]. older and sandier rock formation than the Tanezzuft Formation restricted within the paleo-lows. The Tanezzuft Formation grades up into the overlying Akakus Formation, a regressive unit of fine-grained sandstone that forms a prominent escarpment in outcrop at the western margin of the basin. The Akakus is generally absent in the sub-surface due to truncation at the Caledonian unconformity, which also removed a significant thickness (locally all) of the Tanezzuft Formation [14]. Above this, the Devonian is represented by sequences of shales, sandstones, and minor carbonates. In the basal part of the Devonian interval, two units termed “Basal Devonian Sands” (BDS) I and II have been recognized as secondary reservoir objectives. Both units are separated by extensive regional shale. The BDS section is conformably overlain and maybe, in part, laterally equivalent to the Awaynat Wanin Group. Although this group contains organic-rich shales, they are thermally immature throughout the Murzuq basin. The latest Devonian (Strunian) Tahara Formation, comprising sandstones, rests on a minor disconformity [14].

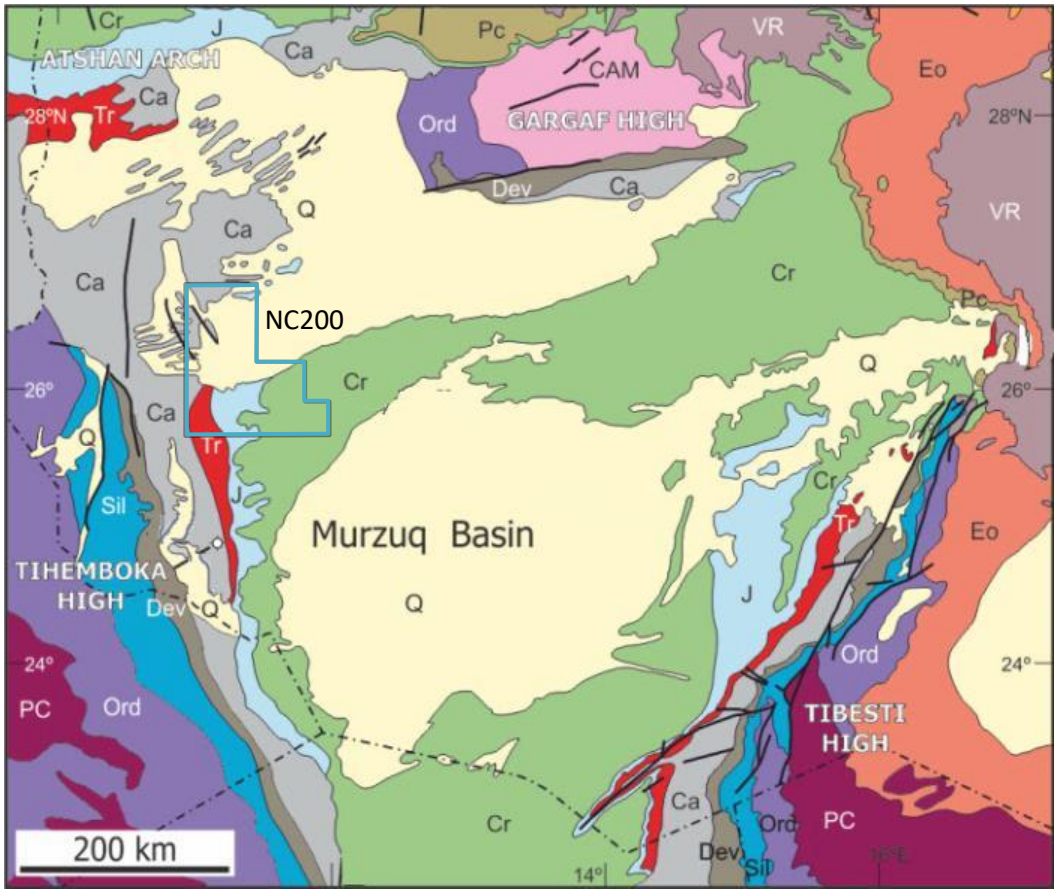

Fig. 1. Geological map of Murzuq basin showing the major stratigraphic units, the basin boundaries, and the location of the Erawin oil field (NC 200) modified from [15]. PC= Precambrian; CAM=Cambrian; Ord=Ordovician; Sil=Silurian; Dev; Devonian; Ca= Carboniferous; Tr= Triassic; J= Jurassic; Cr=Cretaceous; Pc=Paleocene; Eo=Eocene; VR= Tertiary volcanic rocks; and Q=Quaternary

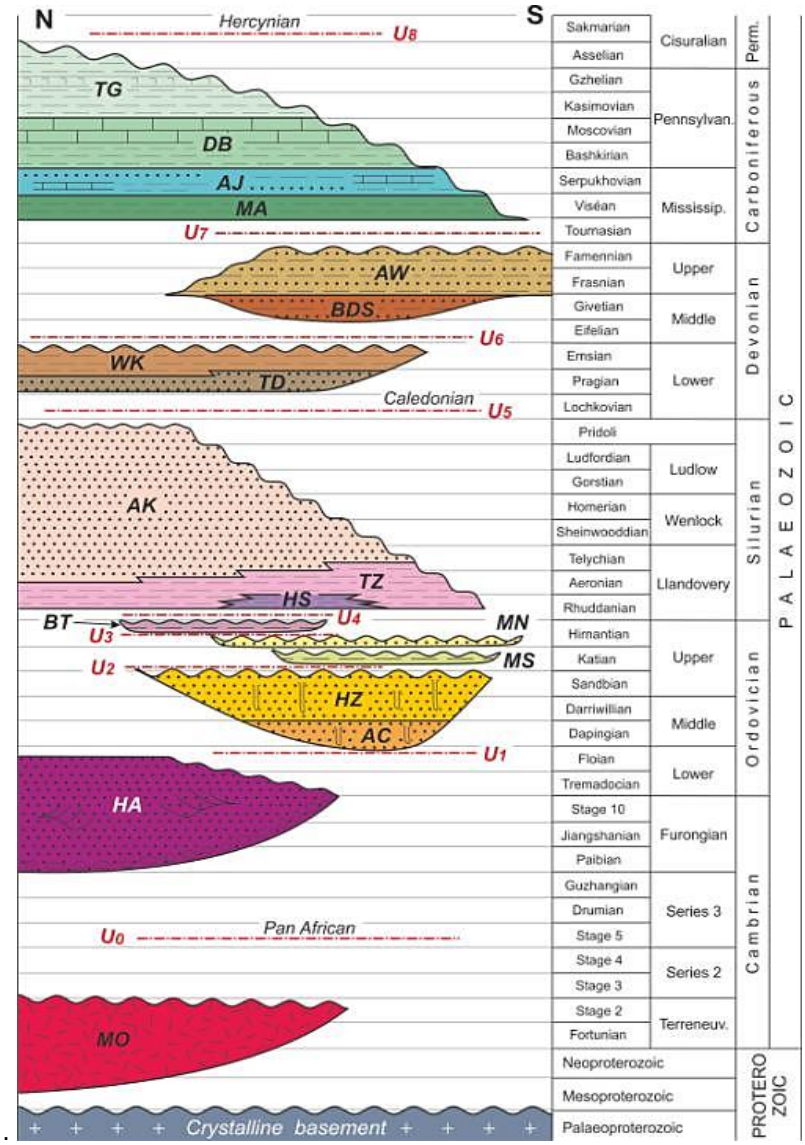

Fig. 2. Generalized chronostratigraphic section of the Murzuq Basin showing the major lithostratigraphic units and their major unconformities (adapted from [15]). MO = Mourizide; HA = Hasawnah; AC = Achabiyat; HA = Hawaz; MS = Melaz Shuqran; MN = Mamuniyat; BT = Bir Tlacsin; HS = Hot Hale; TZ = Tanezzuft; AK = Akakus; TD = Tadrart; WK = Wan Kasa; BDS = Basal Devonian Sandston; AW = Awaynat Wanin; MA = Marar; AJ = Assedjefar; DB =Dembaba; TG = Tiguentourine; and U1-U6 = major unconformities

The Marar Formation is a marine shale with interbedded sandstones (potentially serving as a secondary reservoir target at the northern edge of the basin). The Marar Formation is succeeded by lagoonal mudstones and algal limestones of the Collenia Beds, which the Assedjefar Formation and Dembaba Formation then follow. The Dembaba Formation marks a significant marine transgression in the Murzuq basin and acts as a seismic marker that could be locally truncated at the Hercynian unconformity [11]. The subsequent continental red-bed sequence may contain Upper Carboniferous (Stephanian) at its base but primarily comprises of Triassic, Jurassic, and Lower Cretaceous sediments. The latter are visible in a distinct escarpment at the northern boundary of the basin. The post-Hercynian section has been notably eroded due to the combined impacts of Austrian and late Alpine uplift and erosion. Lastly, in the Quaternary period, Recent Aeolian dune sands and alluvium extensively cover various parts of the basin [16].

Geochemistry: Total organic carbon and Rock-Eval Pyrolysis data are utilized to assess the potential, type, maturity, and hydrocarbon generation of extracted organic matter from sediment samples. Kerogen-types variation is determined based on hydrogen index (HI) versus oxygen index (OI) data in source rocks [13]. The abundance of OM in source rocks can be estimated using a global factor (Barker, 1996). Elevated values (>1.0) for the S_1 peak (free hydrocarbons) and abnormally high PI values (>0.2) suggest migrated bitumen in [8,17]. In the Murzuq Basin, west-south Libya, the lower Silurian shales of the Tanezzuft Formation are identified as the primary source rocks for hydrocarbons in the region [11,14]. In the past decade, significant attention has been given to the remaining Palaeozoic facies by a team of researchers who identified other formations like the Devonian Awaynat Wanin Formation and the Lower Carboniferous Marar Formation as potential source rocks [15,16,18,19]. Their geochemical studies concluded that the predominant kerogen in carboniferous and Devonian formations is type II, mature based on the T_{max} parameter, and capable of producing and expelling liquid hydrocarbons [20]. The maturity parameters such as T_{max}, R_o%, and SCI, along with elevated TOC and dark-grey shale lithology values, indicated contributions from the Upper Devonian Awaynat Wanin Formation and the Lower Carboniferous Marar Formation [16]. Rock-Eval measurements revealed the TOC content and biomarker values from the Devonian and Carboniferous layers of the Paleozoic Era. The data confirmed that these rocks could be potential oil source rocks in the Murzuq Basin [21]. Samples (n = 85) were collected from the Paleozoic formations of Well C1-NC200 and Well D1-NC200 to explore the Erawin Field and Murzuq Basin (Fig. 1).

Objective: The paper aims to understand the geochemical features and potential hydrocarbon accumulation in Paleozoic formations from two wells in the NC 200 Block. Through Rock-Eval analysis, TOC (total organic carbon), and Gas Chromatography-Mass Spectrometry (GC-MS), the research sought to determine the geochemical parameters such as S1 (free hydrocarbons), S2 (total hydrocarbons), and S3 (organic carbon dioxide) to evaluate the hydrocarbon potential, kerogen types, and maturity parameters (Tmax). A molecular composition, including *n*-alkanes, cyclic isoprenoids, biomarkers, and carbon isotopes (δ13C), will be utilized to support these findings.

2. EXPERIMENTAL METHODS

Eighty-five samples, corresponding to the Palaeozoic formations, were taken from two wells in the NC 200 Block of the Murzuq Basin. The Rock-Eval analysis was utilized to determine the parameters for investigating the potential hydrocarbon generation of the organic matter. Crushed samples weighing 100 mg were pyrolyzed at 325°C for 3 minutes in a helium environment before undergoing temperature-programmed pyrolysis at 25°C/min from 300 to 650°C. Hydrocarbons were detected using a flame ionization detector (FID). During isothermal pyrolysis at 300°C, a first peak (S_1 mg HC/g) indicated the volatilization of free hydrocarbons. The second peak (S_2 mg HC/g) resulted from the thermal cracking of kerogen into hydrocarbons at temperatures between 300 and 550°C. An IR detector measured the third peak (S_3), indicating the amount of carbon dioxide produced from one gram of rock during pyrolysis at a temperature between 300°C and 390°C. The highest temperature at which the maximum amount of hydrocarbon can be generated through kerogen cracking is known as T_{max}. The total organic carbon (TOC) organic matter, was determined for each sample using a LECO carbon analyzer.

A droup of samples was carefully selected for further geochemical investigations. The source rocks were extracted by placing approximately 40 g of crushed sample in a pre-weighted thimble covered with pre-extracted glass wool. A mixture of dichloromethane and methanol (93:7) was used in a Tecator Soxtec HT-System for extraction. The samples underwent boiling for one hour, followed by a two-hour rinsing process. The extracted sample was then transferred to a flask using a Buchi rotary evaporator to remove the solvent. Asphaltene was separated from the extracts by precipitating it with *n*-pentane in an ultrasonic bath for three minutes, filtering it with maltene, and transferring it to a pre-weighted glass vial. The saturated fractions were analyzed using a gas chromatograph (GC) equipped with a GC/FID (gas chromatograph with flame ionization detector; DANI 8510) featuring an OV1 (25m) column and FID detector. Helium gas was used as the carrier for the extraction injection. The temperature was programmed to increase by 4°C per minute from 80 to 300°C and maintained for 20 minutes. The temperature program ranged from 40°C to 290°C at a 4°C/min rate, with helium as the carrier gas. The entire hold time was ten minutes. Biomarkers were analyzed using Gas Chromatography-Mass

Spectrometry (GC-MS) with a Hewlett-Packard 5890 gas chromatograph connected to an AutoSpec Ultima system. A fused silica SE54 capillary column (40 m x 0.22 mm i.d.) was installed directly into the ion source. The initial oven temperature of 45°C was held for 1.5 minutes before being increased to 150°C at a rate of 35°C per minute for 14 minutes. The injector and detector were maintained at a temperature of 300 °C. The oven column was directly connected to the ion source through a transfer line operating at 300 °C and the electron impact ion source at 70 eV. The Chemstation software processed the statistics once they were collected in the specified ion monitoring (SIM) mode.

3. RESULTS AND DISCUSSION

The borehole locations, cuttings list, and depths for rock data collection are detailed in Tables 1 and 2. Rock-Eval and TOC data from selected samples were analysed using Rock-Eva pyrolysis and TOC evolution. The Rock-Eval pyrolysis method was initially introduced by [17] and has since undergone various analytical enhancements. Parameters identified through Rock-Eval pyrolysis measurements are crucial [17,22,23]. The findings from Rock-Eval pyrolysis and TOC assessments for the intervals are summarized in Tables 1, 2, and 3. The organic content is a minor component of the sediment bulk, as indicated in Table 3. Key Rock-Eval pyrolysis parameters include S_1 (mg HC/g rock) for free organic matter content (up to approximately C33), S_2 (mg HC/g rock) for total hydrocarbons produced by pyrolysis (including some bitumen), and S_3 (mg CO2/g rock) for organic carbon dioxide released at 390 °C. The maximum temperature (T_{max}) for S_2 yield is in °C. The value of S_2/TOC in mg HC/g rock denotes the hydrogen index (HI), while S_3/TOC signifies the oxygen index (OI), and PI represents the production index (mg CO_2/g rock). Data on these parameters in Tables 2 and 3 will be utilized for correlation and mapping in subsequent sections to unveil the geochemical characteristics of the samples.

Table 1. TOC and Rock-Eval parameters of the source rock samples collected from Bir Tlacsin, Tanezzuft, Awaynat Wanin (Aw. Wa.), Basal Devonian Shale (BDS shale), Basal Devonian Sandstone (BDS II), and Lower Marar Formations from the C1-NC200 Well

Depth ft	Formation	S_1	S_2	S_3	TOC%	Tmax	S_2/S_3	HI	OI	PI
2940	Lwr Mrar	0.1	1.6	0.9	1.90	428	1.8	87	49	0.1
2970	Lwr Mrar	0.3	6.0	1.7	3.70	423	3.5	163	47	0.0
3000	Lwr Mrar	0.2	3.2	1.4	2.30	431	2.3	135	188	0.1
3030	Lwr Mrar	0.2	2.3	1.5	2.20	427	1.5	103	67	0.1
3060	Lwr Mrar	0.1	0.6	0.7	1.30	428	0.9	45	52	0.2
3090	Lwr Mrar	0.1	1.0	0.7	1.40	431	1.5	75	50	0.1
3120	Lwr Mrar	0.2	0.9	0.5	1.30	429	2.0	71	35	0.2
3150	Lwr Mrar	0.2	0.7	0.6	1.00	431	1.1	65	61	0.2
3180	Lwr Mrar	0.1	0.3	0.7	0.60	427	0.5	56	118	0.3
3210	Aw. Wa.	0.1	0.3	0.5	0.50	425	0.6	58	104	0.3
3240	Aw. Wa.	0.2	1.1	4.0	1.10	428	0.3	96	350	0.2
3270	BDS II	0.3	3.6	1.7	2.60	429	2.1	139	66	0.1
3300	BDS shale	0.3	1.7	2.1	1.60	431	0.8	108	130	0.2
3360	Tanezzuft	0.1	0.8	0.8	0.40	430	1.0	203	200	0.1
3480	Tanezzuft	0.1	1.0	0.4	0.40	432	2.6	237	93	0.1
3540	Tanezzuft	0.1	1.4	0.3	0.50	429	4.0	269	67	0.1
3570	Tanezzuft	0.1	1.6	0.4	0.60	430	4.3	267	62	0.0
3600	Tanezzuft	0.1	1.7	0.4	0.60	430	4.7	284	60	0.0
3630	Tanezzuft	0.1	1.3	0.5	0.50	430	2.6	260	102	0.1
3650	Tanezzuft	0.1	1.4	0.4	0.50	433	3.6	271	75	0.1
3670	Tanezzuft	0.1	1.3	0.4	0.50	432	3.1	233	76	0.1
3710	Tanezzuft	0.1	1.2	0.5	0.50	430	2.7	254	96	0.0
3750	Tanezzuft	0.1	1.3	0.4	0.50	430	3.4	271	79	0.1
3810	Tanezzuft	0.1	1.0	0.4	0.40	428	2.4	256	108	0.1
3930	Bir Tlacsin	0.3	1.4	0.9	0.50	434	1.6	262	165	0.2
3980	Bir Tlacsin	0.2	0.8	1.3	0.40	433	0.6	195	325	0.2
4010	Bir Tlacsin	0.3	1.9	2.0	0.70	431	1.0	295	302	0.1
4110	Bir Tlacsin	0.2	1.1	2.1	0.60	433	0.5			0.2

Table 2. TOC and Rock-Eval parameters of the source rock samples collected from Bir Tlacsin, Tanezzuft, Awaynat Wanin (Aw. Wa.), Akakus, Lower Marar, Marar, Marar Carbonates (Marar CB), and Assedjefar Formations from the D1-NC200 Well

Depth ft	Formation	S_1	S_2	S_3	TOC%	T_{max}	S_2/S_3	HI	OI	PI
1500	Assedjefar	0.07	0.74	1.11	1.49	431	0.67	50	74	0.09
1530	Assedjefar	0.06	0.97	0.75	1.47	432	1.29	66	51	0.06
1590	Marar CB	0.08	0.63	0.54	1.44	431	1.17	44	38	0.11
1620	Marar CB	0.06	0.55	0.51	1.56	434	1.08	35	33	0.1
1740	Marar CB	0.04	1.03	0.45	1.86	430	2.29	55	24	0.04
1770	Marar	0.04	1.61	0.60	2.10	433	2.68	77	29	0.02
1800	Marar	0.04	1.50	1.03	2.30	432	1.46	65	45	0.03
1830	Marar	0.07	2.36	0.74	2.96	429	3.19	80	25	0.03
1860	Marar	0.02	1.16	0.55	1.81	432	2.11	64	30	0.02
1890	Marar	0.04	0.88	0.47	1.75	435	1.87	50	27	0.04
1920	Marar	0.02	0.62	0.43	1.46	431	1.44	42	29	0.03
1950	Marar	0.03	0.81	0.56	1.46	431	1.45	55	38	0.04
1980	Marar	0.05	2.35	0.49	2.06	434	4.8	114	24	0.02
2010	Marar	0.08	1.97	0.63	1.85	428	3.13	106	34	0.04
2040	Marar	0.07	1.36	0.58	1.51	432	2.34	90	38	0.05
2070	Marar	0.14	2.93	0.69	2.44	432	4.25	120	28	0.05
2100	Marar	0.05	1.89	0.50	1.78	432	3.78	106	28	0.03
2130	Marar	0.05	1.23	0.49	1.50	433	2.51	82	33	0.04
2160	Marar	0.08	1.72	0.44	1.76	429	3.91	98	25	0.04
2190	Marar	0.07	2.17	0.47	1.80	433	4.62	121	26	0.03
2220	Marar	0.06	1.13	0.45	1.18	433	2.51	96	38	0.05
2250	Lwr Marar	0.07	1.60	0.51	1.77	434	3.14	90	29	0.04
2280	Lwr Marar	0.06	1.66	0.45	1.38	435	3.69	120	33	0.03
2310	Lwr Marar	0.14	4.02	0.58	2.43	431	6.93	165	24	0.03
2340	Lwr Marar	0.1	4.22	0.69	2.69	434	6.12	157	26	0.02
2370	Lwr Marar	0.04	0.77	0.75	1.33	433	1.03	58	56	0.05
2400	Lwr Marar	0.05	0.69	0.52	1.20	432	1.33	58	43	0.07
2430	Lwr Marar	0.02	0.91	0.65	1.58	428	1.4	58	41	0.02
2460	Lwr Marar	0.04	0.70	0.51	1.18	434	1.37	59	43	0.05
2490	Lwr Marar	0.05	0.53	0.34	0.97	432	1.56	55	35	0.09
2520	Lwr Marar	0.02	0.22	0.45	0.71	426	0.49	31	63	0.08
2610	Aw. Wa.	0.04	0.36	0.42	0.75	433	0.86	48	56	0.1
2640	Aw. Wa.	0.04	0.61	0.51	1.11	434	1.2	55	46	0.06
2670	Akakus	0.09	0.62	0.78	1.22	431	0.79	51	64	0.13
3750	Tanezzuft	0.08	2.16	0.39	0.79	433	5.54	273	49	0.04
3780	Tanezzuft	0.12	2.35	0.44	0.86	432	5.34	273	51	0.05
3820	Tanezzuft	0.03	0.66	0.56	0.49	434	1.18	135	114	0.04
3940	Tanezzuft	0.06	0.93	0.49	0.43	437	1.9	216	114	0.06
4030	Tanezzuft	0.05	1.58	0.52	0.53	440	3.04	298	98	0.03
4150	Tanezzuft	0.04	0.64	0.38	0.37	433	1.68	173	103	0.06
4250	Tanezzuft	0.04	0.97	0.30	0.47	438	3.23	206	64	0.04
4350	Tanezzuft	0.06	0.85	0.37	0.39	436	2.3	218	95	0.07
4450	Tanezzuft	0.05	0.98	0.36	0.43	440	2.72	228	84	0.05
4550	Tanezzuft	0.06	1.10	0.30	0.47	439	3.67	234	64	0.05
4660	Tanezzuft	0.06	0.86	0.30	0.42	438	2.87	205	71	0.07
4750	Tanezzuft	0.39	1.43	0.22	0.56	437	6.5	255	39	0.21
4770	Bir Tlacsin	0.33	1.58	0.50	0.55	435	3.16	287	91	0.17
4790	Bir Tlacsin	0.61	2.68	0.40	0.79	436	6.7	339	51	0.19
4820	Bir Tlacsin	0.85	3.49	0.72	0.91	439	4.85	384	79	0.2
4840	Bir Tlacsin	0.32	2.16	0.73	0.71	438	2.96	304	103	0.13
4870	Bir Tlacsin	0.55	2.04	3.02	0.56	433	0.68	364	539	0.21
4880	Bir Tlacsin	0.85	2.25	2.73	0.72	435	0.82	312	379	0.27
4990	Bir Tlacsin	0.04	0.58	0.50	0.36	441	1.16	161	139	0.06
5080	Bir Tlacsin	0.05	0.62	0.44	0.37	443	1.41	168	119	0.07
5140	Bir Tlacsin	0.15	2.78	0.58	1.06	440	4.79	262	55	0.05

TOC and Rock-eval pyrolysis: Twenty-eight samples from Well C1-NC200 were analyzed to determine TOC and Rock-Eval pyrolysis values. The TOC data and Rock-Eval pyrolysis parameters from samples collected from this well are presented in Table 1. Fifty-five samples from Well D1-NC200 were examined to establish TOC values and Rock-Eval data. TOC ratios and Rock-Eval values are illustrated in Table 2. In both wells, TOC values are predominantly above 0.5, as depicted in Fig. 3, indicating three potential source rocks: shales from the Carboniferous Marar/Lower Marar Formations, the Devonian Awaynat Wanin/BDS II Formations, and the Silurian Tanezzuft Formation. The Marar/Lower Marar Formations exhibit kerogen with > 1 TOC% maybe type III or IV kerogen, with most samples showing good to fair potential for source rock accumulation. The shales of the Devonian Awaynat Formations have generally fair to good, slightly lower recovery potential than the Marar Formation. Specifically, B1-NC200 shales demonstrate fair potential with TOC ranging from 1-3%. The data on hydrocarbon potential in this study confirms that the Awaynat Wanin/BDS II Formations have fair potential and may be richer than the Marar/Lower Marar Formations. The TOC values of Tanezzuft and Bir Tlacsin Formations are below 1% in the most intervals, indicating a more mature oil generation stage, which will become more apparent based on maturity parameters. The correlation and presentation of TOC, S_1, S_2, and S_3 data reveal varying hydrocarbon generation potential and different levels of thermal maturity among formations in both wells. However, the carboniferous Marar/Lower Marar Formations in both wells showed the highest readings of TOC and S_2. In Well C1-NC200 at 2970 ft and 3000 ft, the S_2 recorded 6 and 3.2, associated with TOC 3.7 and 2.3, respectively. Similarly, in Well D1-NC200 at the depths of 2310 ft and 2340 ft, the S_2 showed 4.02 and 4.22 and TOC 2.43 and 2.69, reflected in the S_2/S_3 values (the tables) as the highest values. The significance of these values confirms other hydrocarbon sources exist, as multi-unconventional source rocks may mature less than those known.

Kerogen types: The conversion of organic matter through the burial process into kerogen, then oil and gas, has been extensively studied. Gas matter is mainly produced through a biogenic and thermogenic process, formed by anaerobic micro-organisms during the initial diagenetic burial stage or from bacteria-laden water. Four types of kerogens are identified. Type I has high hydrogen and low oxygen content; Type II is derived from protein and lipid-rich sources; Type III originates from environments rich in terrestrial plants with more oxygen than hydrogen; and Type IV kerogen is the residual deposit from pre-existing kerogen that has undergone full maturation [13]. The Hydrogen Index (HI) (S_2/TOC) indicates of kerogen type, as shown in Fig. 4, where multiple kerogen types are depicted and categorized based on HI values. Type IV, Type III, Type II/III, and Type II kerogens correlate with increasing depth, indicating the age of formations ranging from Type II as protein and lipid in early stages to Type III kerogens from terrestrial plants and Type IV from residual deposits.

T_{max} as maturity parameter: T_{max} is the maximum temperature at which most hydrocarbons are produced in the Rock-Eval pyrolysis. According to most researchers, T_{max} values less than 425 °C are considered immature; the oil generation window commences at 430 °C; early mature oil is at 435–440 °C; and late mature oil between 440 and 460 °C [13]. Furthermore, T_{max} values greater than 470 °C are considered as over-mature and may produce a wet or dry gas from Type II kerogen [24]. Consequently, the T_{max} data from this search agrees with the facts above. Commonly, the formations in both wells are mature and deeper, as shown in Fig. 5. The depths of well D1 may be a reason for higher hydrocarbon maturity than well C1. This fact appears even between the same formations, as the highest T_{max} of the C1 well was less than 435 °C, while some T_{max} from the D1 well samples was more than 440 °C. In fact, many levels of maturity can be seen, from immature to early mature, and it is not accurate to report that the maturity of any formation can be evaluated based on a limited number of wells even in the same concession. This is strongly clear in Fig. 5. For example, the T_{max} data of the Marar/Lower Marar formation showed a great difference between the studied wells regarding maturity and formations in the same boat. Based on the T_{max} parameter for both wells, the maturity ranges from immature to late mature, as facts confirm conclusions that multi-source generation may be unconventional, as published by several of authors [16,18,20].

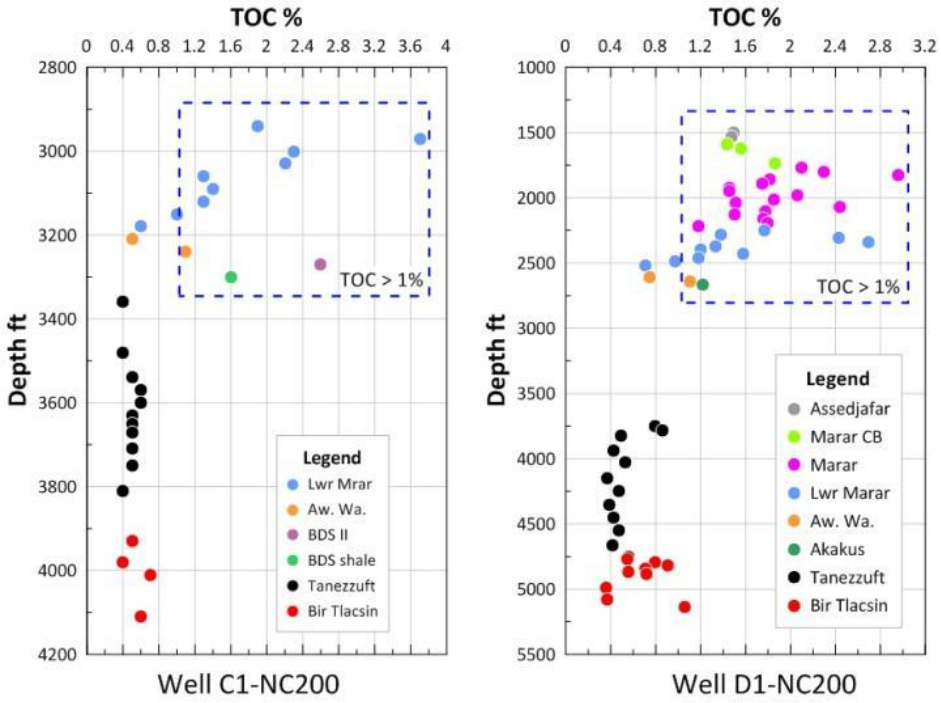

Fig. 3. Distributions of Total Organic Content (TOC) in the examined wells indicate that the amount of organic matter in Silurian source Rocks is notably lower than in the Devonian-Carboniferous sources

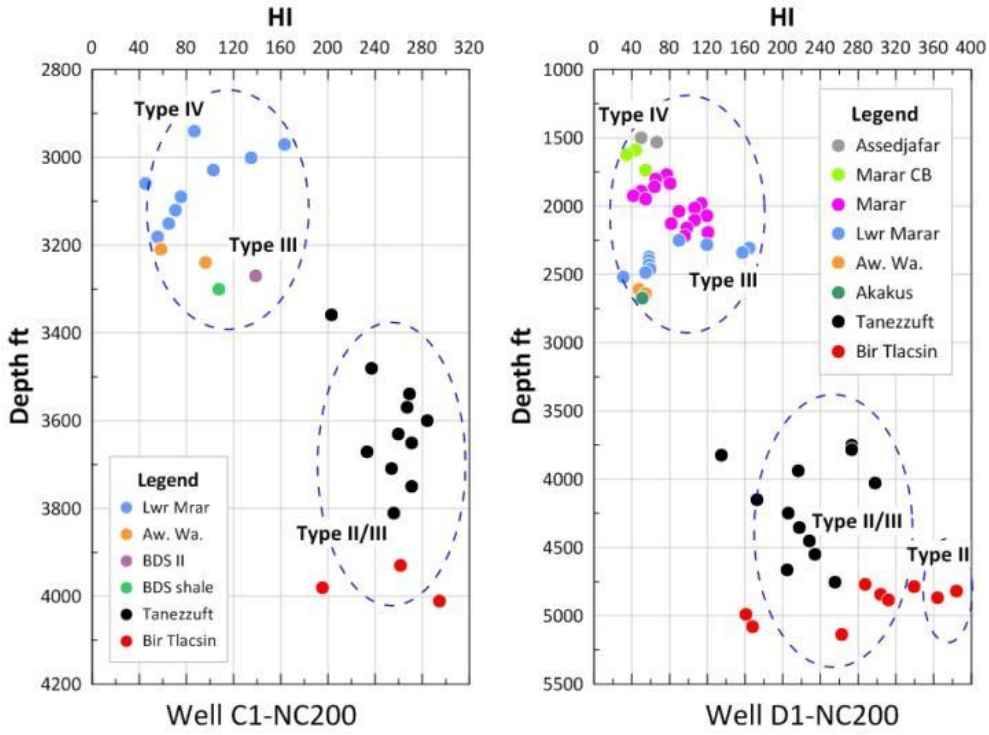

Fig. 4. The HI values of the selected samples from both C1- and D1-NC200 wells plotted verses the depth showing the Silurian sources are mostly represented by type II/III kerogen and minor type II kerogen (in D1-NC200, particularly), In contrast, type III and IV kerogen dominate the Devonian-Carboniferous source rocks

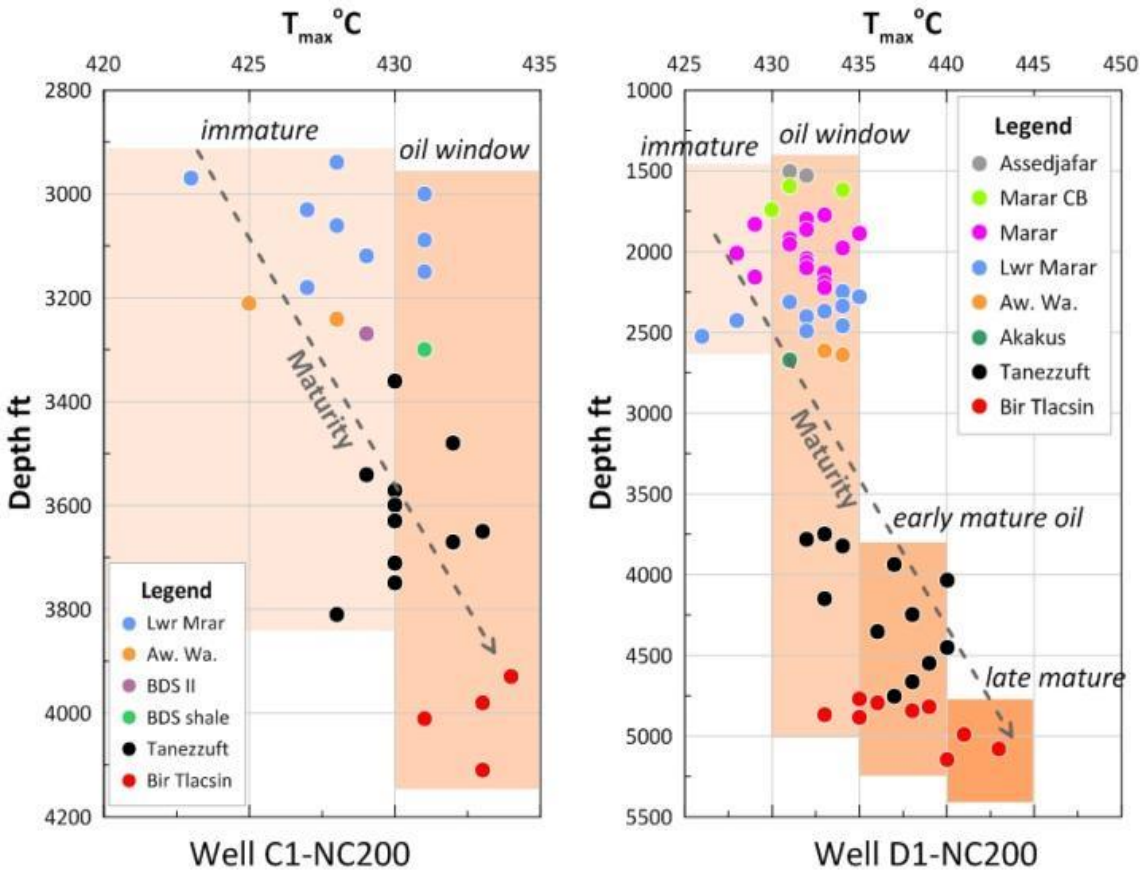

Fig. 5. The T_{max} maturity parameter of the samples collected from the C1- and D1-NC200 shows that the samples of Silurian Source rocks located at the oil window at least, while the Devonian Carboniferous Sources were immature to the oil window maximum

3.1 Molecular Composition

***n*-alkanes and cyclic isoprenoids:** The biomarker compounds are highly informative and can be applied geochemically to study petroleum geochemistry, including steroids, *n*-alkanes, isoprenoids, and terpenoids [25]. The *n*-alkanes have long been used as indicators due to their abundance and ease of differentiation using geochemical techniques such as gas chromatography (GC) or gas chromatography mass-spectrometry GC-MS; [26]. Also, they are characterized by a simple carbon chain structure based on chemical formula of C_nH_{2n+2}. GC-MS also identifies the n-alkanes based on the m/z 85 fragment. The fingerprints *n*-alkanes can be influenced by factors such as biological input and maturity level, which are controlled and reflected in the distributions of *n*-alkanes [27].

The saturated hydrocarbon gas chromatogram of the selected samples with a high EOM content reveals different *n*-alkane patterns in most formations in both wells. Two samples from the Lower Marar formation (C1 well 2970ft depth and D1 well at depth 2340ft) and four samples from the Tanezzuft Shale (3270ft, 3600ft from C1 well and 3780ft, 4750 ft from D1 well) [28]. The Lower Marar and Tanezzuft Formations, among others, exhibit distinct *n*-alkane profiles, as shown in Fig. 6, including n-C20 and isoprenoids (Pristane & Phytane) compared to *n*-alkane patterns. Therefore, the influence of maturity and kerogen type as the source can be observed through the distributions of *n*-alkanes Fig. 6, consistent with the discussion above that interpreted Rock-Eval pyrolysis. The *n*-alkanes distribution from C_{14}–C_{34} with high peaks at nC_{16} and nC_{17}, indicate to a dominance of marine sources and little input of terrigenous organic matter [29].

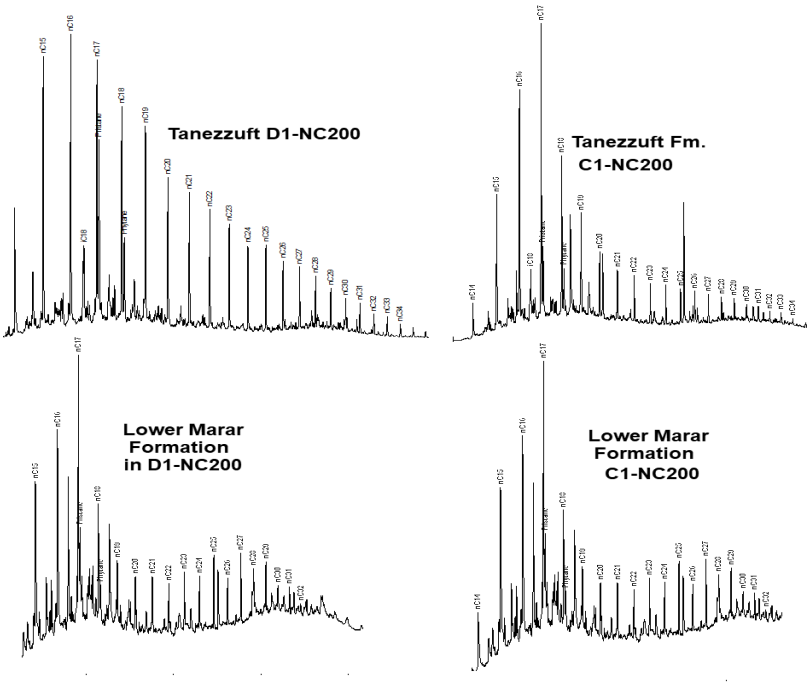

Fig. 6. shows the GC-MS profile of samples from the C1—and D1-NC200 wells of the Silurian (Tanezzuft) and Devonian (Lower Marar) formations. This indicates that the n-C20 and isoprenoids (Pristane & Phytane) exhibit similar patterns to other regular n-alkanes

Biomarker analysis: Numerous researchers have recognized bacterial triterpenoids as precursors of triterpene biomarkers, and various microorganisms in different depositional environments can produce a diverse range of triterpenoids [28]. The primary triterpenoids detected in most geological samples are $\alpha\beta C_{29}$ and $\alpha\beta C_{30}$ hopanes [28]. Gas chromatograph-mass spectrometry analyzed using a GC-MS chromatograph oven programmed in full scan (TIC) mode. Steranes are biomarkers derived from higher plants, animals, and algae; however, they are uncommon in prokaryotic organisms [29]. GC-MS can distinguish Sterane biomarkers using fragmentograms like m/z 217 for steranes, m/z 231 for methyl steranes, and m/z 259 for diasteranes [28]. Steranes are composed of saturated tetracyclic-structured hydrocarbons, with six isoprene subunits totalling 30 carbon atoms [25]. Selective ion monitoring (SIM) was utilized to identify terpenes and steranes, by monitoring m/z 191 and 217 (Fig. 7).

Steranes consist of saturated tetracyclic-structured hydrocarbons, with six isoprene subunits totaling 30 carbon atoms [25]. Fig. 7 the mass chromatograms (m/z 191 and 217) show in similar distributions of biomarker fingerprints as indicator of comparable source input. The ratio of *n*-alkane isoprenoid, terpene and sterane as parameters to understand geochemical characteristics of organic matter and to describe the source rocks contributions in Table 3. Geochemical parameters of palaeoenvironments from the distribution and abundance of aliphatic isoprenoids for studied formations such as Pr/Ph = pristane/phytane; Ts/Ts+Tm = ratio of C27 18α(H)-22,29,30-trisnorneohopane/ C27 18α(H)-22,29,30trisnorneohopane + C27 17α(H)-22,29,30-trisnorhopane; C29 αβ/C30αβ = ratio of C29 αβ-hopane / C30 αβ-hopane; S/S+R = ratio of C32 αβ homohopane 22S/ C32 αβ-homohopane 22S + 22R; C23Tr/C30αβ = C23 tricyclic terpane /C30 αβ-hopane, C30βα/C30αβ = C30 βα-hopane /C30 αβ-hopane; $20\Sigma/(20\Sigma+20P)$= C29 αα-sterane 20S/C29 αα-sterane are shown in Table 3. Pristine to Phytane ratios of can be used to identify source lithofacies of organic matter. All the Pr/Ph ratios are showing to have originated from marine shale deposited under sub-oxic conditions (Pr/Ph = 1–2). Based on Ts/Ts + Tm and αααC_{29}20S/20S + 20R parameters, the Tanezzft shale samples more maturity than the rest samples from other formations (Table 3) [30].

Table 3. Geochemical parameters of palaeoenvironments from the distribution and abundance of aliphatic isoprenoids for studied formations

Well	Dept (ft)	Pr/Ph	Ts/(Ts + Tm)	$C_{29}\alpha\beta/C_{30}\alpha\beta$	$C_{32}S/(S+R)$	$C_{23}Tr/C_{30}\alpha\beta$	$C_{30}\beta\alpha/C_{30}\alpha\beta$	$20\Sigma/(20\Sigma+20P)$
C1-NC200	2970		0.28	0.59	0.23	0.22	0.49	0.15
C1-NC200	3270	1.72	0.32	0.47	0.29	0.07	0.34	0.12
C1-NC200	3600		0.45	0.57	0.44	0.11	0.21	0.10
D1-NC200	2340		0.24	0.57	0.35	0.04	0.43	0.16
D1-NC200	3780	1.87	0.41	0.71	0.58	0.07	0.18	0.23
D1-NC200	4750	1.86	0.17	0.53	0.60	0.52	0.12	0.45

Pr/Ph = pristane/phytane; CPI = Carbon Preference Index ; Ts/Ts+Tm = ratio of C_{27} 18α(H)-22,29,30-trisnorneohopane/ C_{27} 18α(H)-22,29,30trisnorneohopane + C_{27} 17α(H)-22,29,30-trisnorhopane; C_{29} αβ/C_{30}αβ = ratio of C_{29} αβ-hopane / C_{30} αβ-hopane; S/S+R = ratio of C_{32} αβ homohopane 22S/ C_{32} αβ- homohopane 22S + 22R; C_{23}Tr/C_{30}αβ = C_{23} tricyclic terpane /C_{30} αβ-hopane, C_{30}βα/C_{30}αβ = C_{30} βα-hopane /C_{30} αβ-hopane; $20\Sigma/(20\Sigma+20R)$ = C_{29} αα-sterane 20S/C_{29} αα-sterane

Table 4. The isotopic composition of the extracted organic matter, and saturate and aromatic fractions

Well name	Depth (Ft)	EOM ‰	Sat. ‰	Aro. ‰
	2970	-27.52		
C1-NC200	3270		-30.12	-28
	3600	-29.77		
	2340	-26.97		
D1-NC200	3780		-30.64	-30
	4750		-30.06	-30

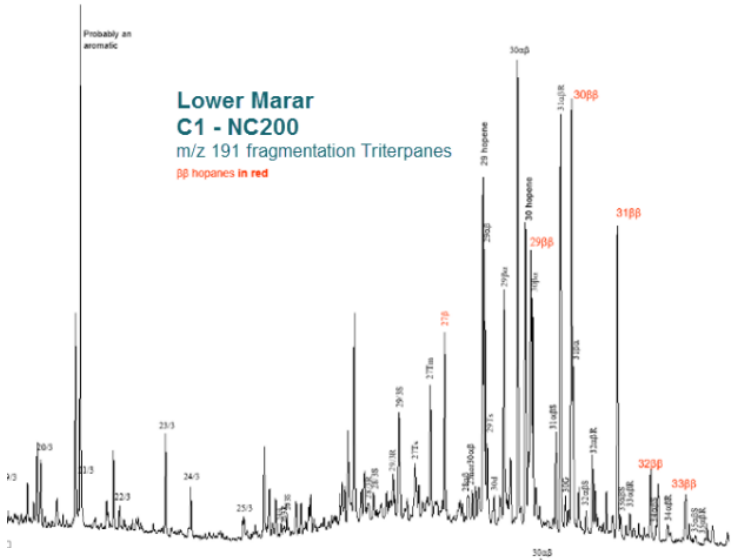
Probably an aromatic
Lower Marar
C1 - NC200
m/z 191 fragmentation Triterpanes
ββ hopanes in red
30αβ
29 hopene
30 hopene
30ββ
29ββ
31ββ
32ββ
33ββ

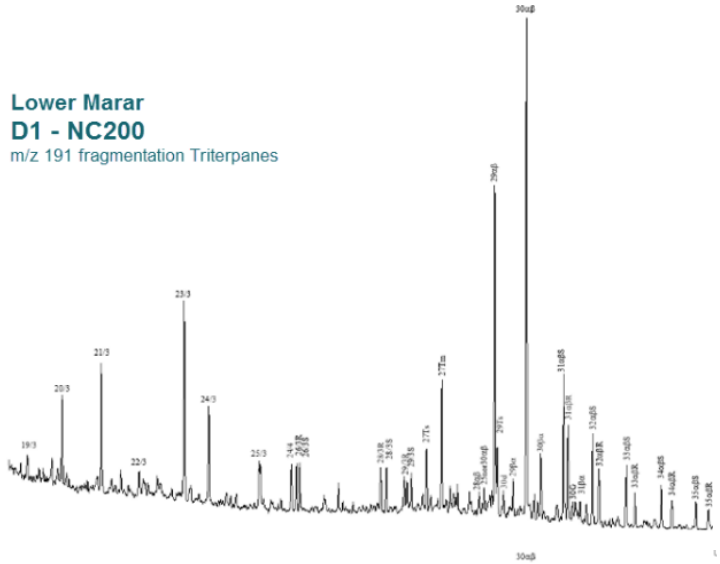
Lower Marar
D1 - NC200
m/z 191 fragmentation Triterpanes
30αβ

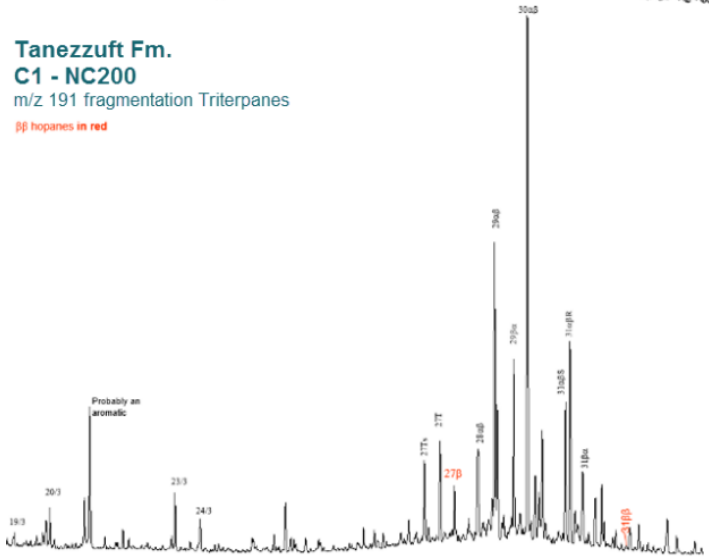
Tanezzuft Fm.
C1 - NC200
m/z 191 fragmentation Triterpanes
ββ hopanes in red
Probably an aromatic
30αβ
27β
31ββ

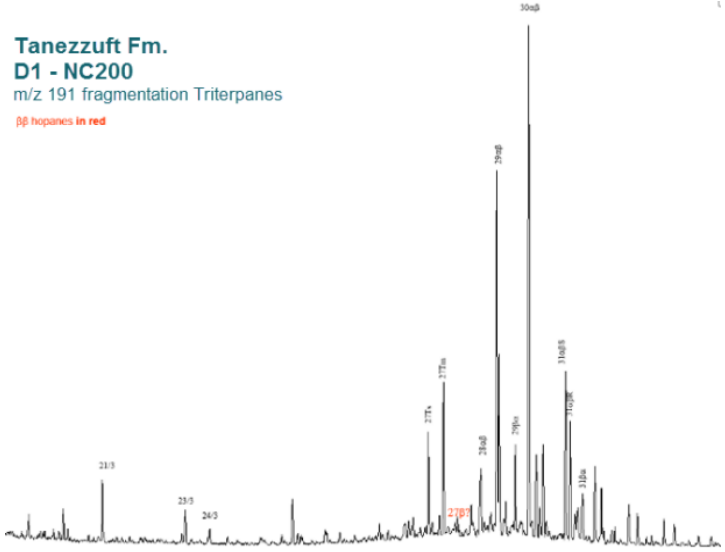
Tanezzuft Fm.
D1 - NC200
m/z 191 fragmentation Triterpanes
ββ hopanes in red
30αβ

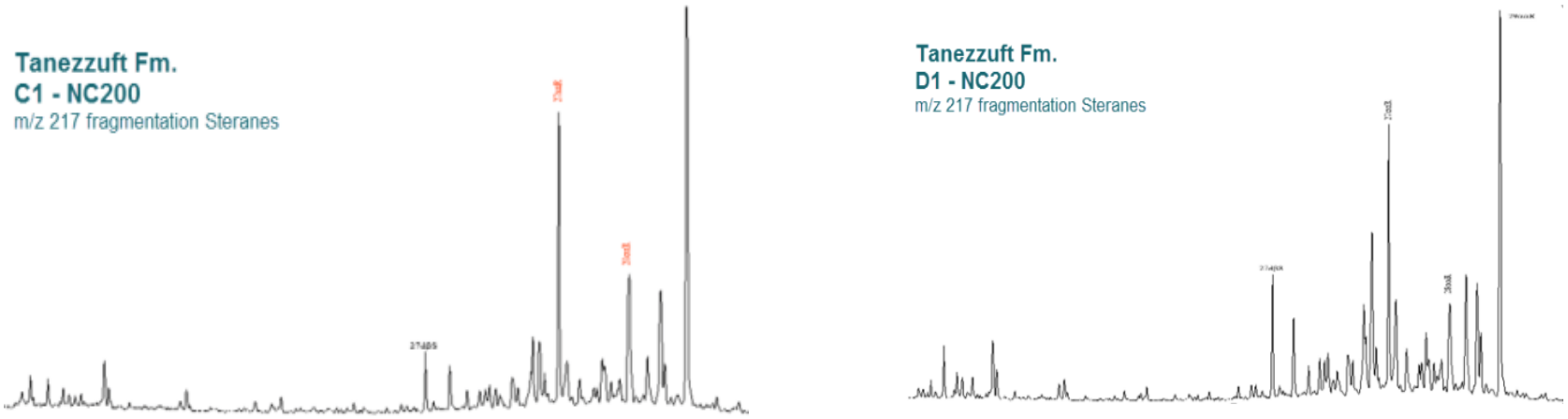

Fig. 7. Mass chromatogram (m/z 191 and m/z 217) of the lower Marar and Tanezzuft Formations shows the distribution of the Triterpanes and steranes

Carbon isotopes ($\delta^{13}C$): The carbon isotope data are presented in Table 4 for selected samples from wells C1-NC200 and D1-NC200. The average $\delta^{13}C$ values of n-alkanes (C15–C30) range from organic matter (EOM) -26.97 to 29.77 ‰, saturated ranges -28.26 to -30.64 ‰, and aromatic ranges -28.00 to -30.00 ‰ (Table 4). It is noted that the $\delta^{13}C$ values from the samples in both wells are relatively more positive, consistent with the explanation of the geochemical characteristics mentioned earlier. The variation of ^{13}C data between the samples (greater than 2‰) cannot be solely attributed to maturity. This mainly reflects differences in source [27,31,32]. Interestingly, the carbon isotope values indicate multiple contributing sources ranging from kerogen Type I to Type III kerogens such as terrestrial plants, with the remaining deposit in Type IV [30]. This strongly supports the arguments presented in the preceding sections.

4. CONCLUSION

The geological setting of the Murzuq Basin in west-south Libya reveals a complex history marked by significant tectonic phases, which have shaped the region's stratigraphy and compositionover millions of years. The Palaeozoic formations, from the Cambrian to the Carboniferous, represent a diverse sedimentary environment ranging from marine to continental, each contributing to the area's rich hydrocarbon potential.

The detailed analysis of the stratigraphic units, conducted through Rock-Eval pyrolysis, Total Organic Carbon (TOC) assessment, and molecular composition studies, has unveiled valuable insights into the basin's hydrocarbon prospectivity. The Lower Carboniferous Marar Formation, the Devonian Awaynat Wanin Formation, and the Silurian Tanezzuft Formation emerge as primary sources of hydrocarbons, with their organic-rich shales displaying favorable characteristics for oil generation.

Furthermore, determining of kerogen types and maturity parameters such as Tmax has provided crucial information about the formations' thermal history and hydrocarbon generation potential. The presence of Type II kerogens in the Silurian Bir Tlacsin and Tanezzuft layers suggests a favorable environment for oil generation, corroborated by elevated TOC values and biomarker analysis.

The carbon isotopes ($\delta^{13}C$) data indicate a multi-contributory source for hydrocarbons, ranging from Type I to Type III kerogens, further emphasizing the complexity of hydrocarbon generation processes in the basin.

DISCLAIMER (ARTIFICIAL INTELLIGENCE)

Author(s) at this moment declare that no generative Artificial intelligence (AI) technologies such as Large Language Models (ChatGPT, COPILOT, etc) and text-to-image generators have been used during the writing or editing of this manuscript.

COMPETING INTERESTS

Authors have declared that they have no known competing financial interests or non-financial interests or personal relationships that could have appeared to influence the work reported in this paper.

REFERENCES

1. Davidson L, Beswetherick S, Craig J, Eales M, Fisher A et al. The structure, stratigraphy and petroleum geology of the Murzuq Basin, southwest Libya. In Geological exploration in Murzuq basin, Elsevier. 2000;295-320.
2. Gurney J. Libya-the political economy of oil; 1996.
3. Caby R, Bertrand J, Black R. Pan-African ocean closure and continental collision in the Hoggar-Iforas segment, central Sahara. In Developments in precambrian geology. Elsevier. 1981;4: 407-434.
4. Vail J. In The Precambrian tectonic structure of north Africa, Symposium on the geology of Libya. 1991;2259-2268.
5. Boullier AM. The pan-African trans-Saharan belt in the Hoggar shield (Algeria, Mali, Niger): A review. The West African orogens and circum-Atlantic correlatives. 1991;85-105.
6. Black R, Latouche L, Liégeois JP, Caby R, Bertrand JM. Pan-African displaced terranes in the Tuareg shield (central Sahara). Geology. 1994;22(7):641-644.
7. Greiling R, Abdeen M, Dardir A, El Akhal H, El Ramly M, El Din Kamal G, Osman AF, Rashwan A, Rice A, Sadek M. A

structural synthesis of the Proterozoic Arabian-Nubian Shield in Egypt. Geologische Rundschau. 1994;83:484-501.

8. Jacobs J, Thomas RJ. Himalayan-type indenter-escape tectonics model for the southern part of the late Neoproterozoic–early Paleozoic East African–Antarctic orogen. Geology. 2004;32(8):721-724.
9. Jacqué M. Reconnaissance géologique du Fezzan oriental. Compagnie française des pétroles; 1962.
10. Billeni E, Massa D. A Stratigraphic Contribution to the Palaeozoic of the Southern Basins. 1980.
11. Hallett, D.; Clark-Lowes, D., Petroleum geology of Libya. Elsevier; 2017.
12. Burollet P, Byramjee R. In Sedimentological remarks on lower palaeozoic sandstones of south Libya, Geology, archaeology and prehistory of the southwestern Fezzan, Libya, Petroleum Exploration Society of Libya, eleventh annual field conference. 1969;91-102.
13. Horsfield B, Curry D, Bohacs K, Littke R, Rullkötter J, Schenk H et al. Organic geochemistry of freshwater and alkaline lacustrine sediments in the Green River Formation of the Washakie Basin, Wyoming, USA. Organic Geochemistry. 1994;22(3-5):415-440.
14. Aziz A. Stratigraphy and hydrocarbon potential of the Lower Palaeozoic succession of License NC-115, Murzuq Basin, SW Libya. In Geological exploration in Murzuq basin, Elsevier. 2000;349-368.
15. Shalbak FA. Palaeozoic petroleum systems of the Murzuq Basin, Libya; 2015.
16. Aboglila S, Albaghdady A, Farifr E, Alborky A. Petroleum geochemistry regional study of Murzuq Basin: Insights from biomarkers characteristic, stable carbon isotope and environmental characterization. Petroleum & Petrochemical Engineering Journal; 2020.
17. Espitalié J, Laporte JL, Madec M, Marquis F, Leplat P, Paulet J, Boutefeu A. Méthode rapide de caractérisation des roches mètres, de leur potentiel pétrolier et de leur degré d'évolution. Revue de l'Institut français du Pétrole. 1977;32(1):23-42.
18. Aboglila S, Ramadan M, Alburki A, Albaghdady A. Biogeochemical analyses of four crude oil samples to confirm the presence of terrestrial-organic matter, collected from the murzuq Basin-Libya. Advances in Research. 2020;21(3):43-50.
19. Aboglila S, Abdulgader A, Albaghdady A, Hlal O, Farifr E, Biomarker ratios and stablecarbon isotopes to describe crude oils characteristics in the Murzuq Basin (Libya). Advances in Research. 2019; 18(3):1-12.
20. Aboglila S, Elaalem M, Ezlit Y, Farifr E. Geochemical characteristics of six formations based on organic geochemical parameters. Murzuq Basin, Libya. Advances in Research. 2018;4:1-11.
21. Albaghday A, Aboglila S, Hlal O, Targhi MH, Farifr E, Sultan MA. Organic geochemical evaluation of the middle devonian to late carboniferous source rocks, South East Murzuq Basin, SW Libya.
22. Tissot BP, Welte DH, Tissot BP, Welte DH., Kerogen: composition and classification. Petroleum formation and occurrence. 1984;131-159.
23. Peters KE. Guidelines for evaluating petroleum source rock using programmed pyrolysis. AAPG bulletin. 1986;70(3):318-329.
24. Madec M, Espitalié J. Determination of organic sulphur in sedimentary rocks by pyrolysis. Journal of Analytical and Applied Pyrolysis. 1985;8:201-219.
25. Peters KE, Moldowan JM. The biomarker guide: interpreting molecular fossils in petroleum and ancient sediments; 1993.
26. Philp R. Fossil fuel biomarkers, methods in geochemistry and geophysics. Elsevier, New York. 1985;23:292.
27. Large D, Gize A. Pristane/phytane ratios in the mineralized Kupferschiefer of the Fore-Sudetic Monocline, southwest Poland. Ore Geology Reviews. 1996;11(1-3):89-103.
28. Waples DW, Machihara T. Biomarkers as Maturity Indicators: Chapter 4; 1991.
29. Volkman JK. A review of sterol markers for marine and terrigenous organic matter. Organic Geochemistry. 1986;9(2):83-99.

30. Goossens Hd, De Leeuw J, Schenck P, Brassell S. Tocopherols as likely precursors of pristane in ancient sediments and crude oils. Nature. 1984; 312(5993):440-442.

Peer-review history:
The peer review history for this paper can be accessed here:
https://www.sdiarticle5.com/review-history/124326